

Crossover in the nature of the metallic phases in the perovskite-type $R\text{NiO}_3$

K. Okazaki,¹ T. Mizokawa,¹ A. Fujimori,¹ E. V. Sampathkumaran,² M. J. Martinez-Lope,³ and J. A. Alonso³

¹Department of Physics and Department of Complexity Science and Engineering, University of Tokyo, Bunkyo-ku, Tokyo 113-0033, Japan

²Department of Condensed Matter Physics and Materials Science, Tata Institute of Fundamental Research, Colaba, Mumbai 400-005, India

³Instituto de Ciencia de Materiales de Madrid, CSIC, Cantoblanco, E-28049 Madrid, Spain

(Received 22 March 2002; revised 12 August 2002; published 6 February 2003)

We have measured the photoemission spectra of $\text{Nd}_{1-x}\text{Sm}_x\text{NiO}_3$, where the metal-insulator transition and the Néel ordering occur at the same temperature for $x \leq 0.4$ and the metal-insulator transition temperature (T_{MI}) is higher than the Néel temperature for $x \geq 0.4$. For $x \leq 0.4$, the spectral intensity at the Fermi level is high in the metallic phase above T_{MI} and gradually decreases with cooling in the insulating phase below T_{MI} while for $x > 0.4$ it shows a pseudogaplike behavior above T_{MI} and further diminishes below T_{MI} . The results clearly establish that there is a change in the nature of the electronic correlations in the middle ($x \sim 0.4$) of the metallic phase of the $R\text{NiO}_3$ system.

DOI: 10.1103/PhysRevB.67.073101

PACS number(s): 71.30.+h, 71.27.+a, 75.30.Kz, 79.60.-i

Many 3d transition-metal compounds undergo a metal-insulator transition as a function of temperature, carrier concentration, bandwidth, and so on.^{1,2} In these systems, electron correlation generally plays an important role. V_2O_3 , $\text{NiS}_{2-x}\text{Se}_x$, NiS, and $R\text{NiO}_3$ (R : rare earth) are well-known *bandwidth-controlled* metal-insulator transition systems. They undergo a transition from an antiferromagnetic insulator to a paramagnetic metal under high pressure or under “chemical pressure.” To understand their phase diagrams from a microscopic point of view is one of the major goals in the studies of strongly correlated systems and much theoretical effort has been made so far along this direction.^{3,4} In V_2O_3 (Ref. 5) and $\text{NiS}_{2-x}\text{Se}_x$,⁶ the metallic phase exists on the lower temperature side of the paramagnetic insulating phase as predicted theoretically³ and as expected from the large magnetic entropy in the paramagnetic insulating phase. On the other hand, the phase diagram of $R\text{NiO}_3$ has a peculiar feature that the metallic phase exists on the higher temperature side of the paramagnetic insulating phase as shown in Fig. 1.⁷

The perovskite-type oxide $R\text{NiO}_3$ belongs to the charge-transfer regime of the Zaanen-Sawatzky-Allen (ZSA) diagram,⁸ and its ligand-to-metal charge-transfer energy Δ is smaller than the 3d-3d Coulomb repulsion energy U ($\Delta < U$). Hence its band gap is given by $\sim \Delta - W$, where W is the one electron bandwidth. Here, W is the width of the hybridized Ni 3d e_g -O 2p σ band. W depends on the Ni-O-Ni bond angle θ through $W \propto \cos^2 \theta$, and hence on the tolerance factor $t [\equiv d_{R-O} / \sqrt{2} d_{Ni-O}]$.⁹ When the rare-earth ionic radius becomes smaller and the crystal structure is more distorted, θ and t become smaller than the ideal value of 180° and 1, respectively. Hence whether the band gap is open ($\Delta \geq W$) or closed ($\Delta \leq W$) is determined by the degree of deviation of θ from 180°. As illustrated in Fig. 1, the least distorted LaNiO_3 , which has the perovskite structure with a weak rhombohedral distortion, is a paramagnetic metal at all temperatures. The other $R\text{NiO}_3$ members, which have the orthorhombic GdFeO_3 -type structure, undergo a temperature-induced metal-insulator transition. The metal-insulator transition and the antiferromagnetic ordering occur at the same temperature for $R = \text{Pr}$ and Nd , while the metal-

insulator transition temperature (T_{MI}) is higher than the Néel temperature (T_N) for the compounds with $R = \text{Sm}$ and other small rare earths. As a result, the metallic phase exists on the higher temperature side of the paramagnetic insulating phase. The boundary between these two types of phase transitions is located between NdNiO_3 and SmNiO_3 . In the $\text{Nd}_{1-x}\text{Sm}_x\text{NiO}_3$ system, $T_{MI} > T_N$ for $x \geq 0.4$, while $T_{MI} = T_N$ for $x \leq 0.4$ (Fig. 1).

Recently, Vobornik *et al.*¹⁰ reported that the temperature dependence of photoemission spectra near E_F in the insulating phase is different between NdNiO_3 and SmNiO_3 , which is probably related with the different magnetoresistance behaviors reported by Mallik *et al.*¹¹ In this paper, we report on a systematic photoemission study of $\text{Nd}_{1-x}\text{Sm}_x\text{NiO}_3$ as a function of x and temperature and indeed reveal quite different behaviors between $x \leq 0.4$ and $x > 0.4$. Based on this result, we propose that there is a phase boundary or a crossover line within this series, which separates the two different kinds of metallic phases in the $R\text{NiO}_3$ system.

Preparation and characterization of polycrystalline

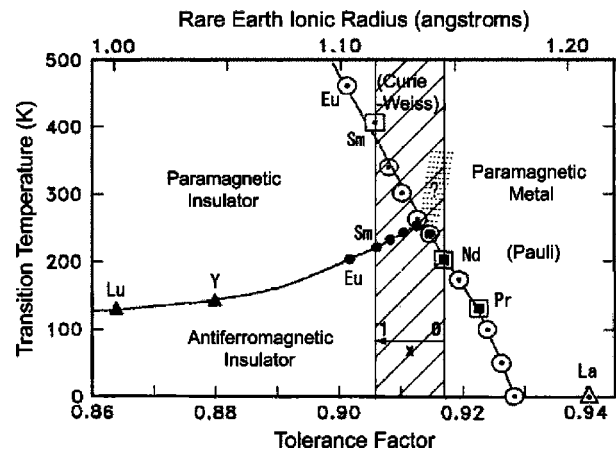


FIG. 1. Phase diagram of $R\text{NiO}_3$ taken from Ref. 7. The hatched area indicates the composition range for which we have measured the photoemission spectra and the dashed lines indicates a new crossover or phase boundary line in the metallic phase proposed in this study.

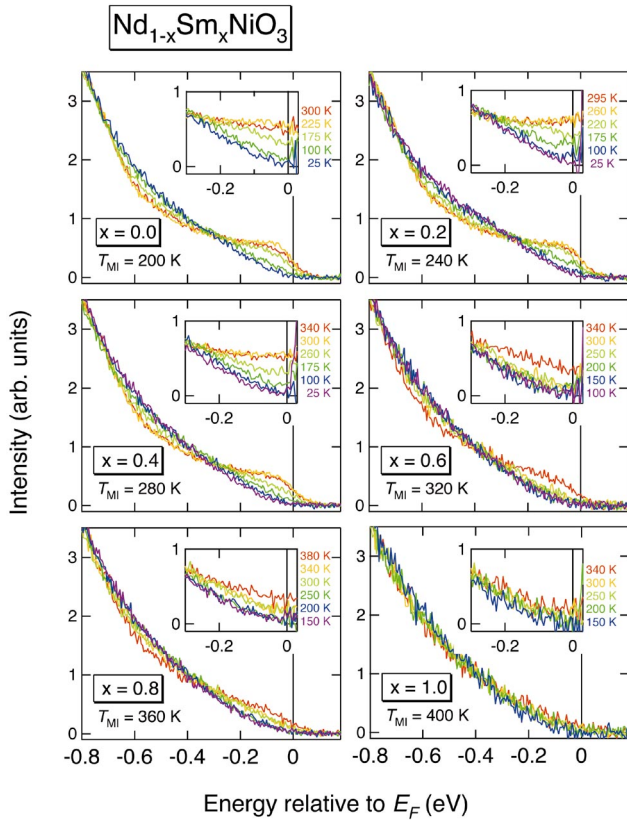


FIG. 2. (Color) Temperature dependence of photoemission spectra in $\text{Nd}_{1-x}\text{Sm}_x\text{NiO}_3$ for various x 's. The inset for each panel shows spectra divided by the Fermi-Dirac function.

$\text{Nd}_{1-x}\text{Sm}_x\text{NiO}_3$ ($x=0.0, 0.2, 0.4, 0.6, 0.8, 1.0$) are described elsewhere.¹¹ The T_{MI} was measured by the differential scanning calorimetric method, and was 199.5 K for NdNiO_3 and 400.2 K for SmNiO_3 . For the T_{MI} of the intermediate compositions, we have linearly interpolated between NdNiO_3 and SmNiO_3 according to Frand *et al.*¹² We have checked the accuracy of this estimate by measuring the T_{MI} of $x=0.6$ to be 324.4 K, which is higher than the interpolated value only

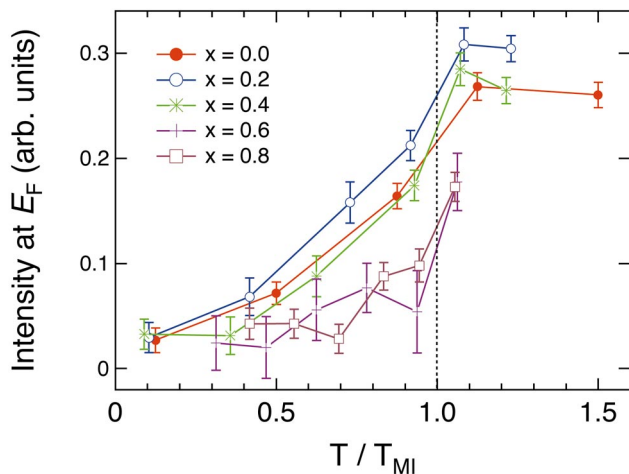


FIG. 3. (Color) Normalized photoemission intensity at E_F as a function of normalized temperature T/T_{MI} .

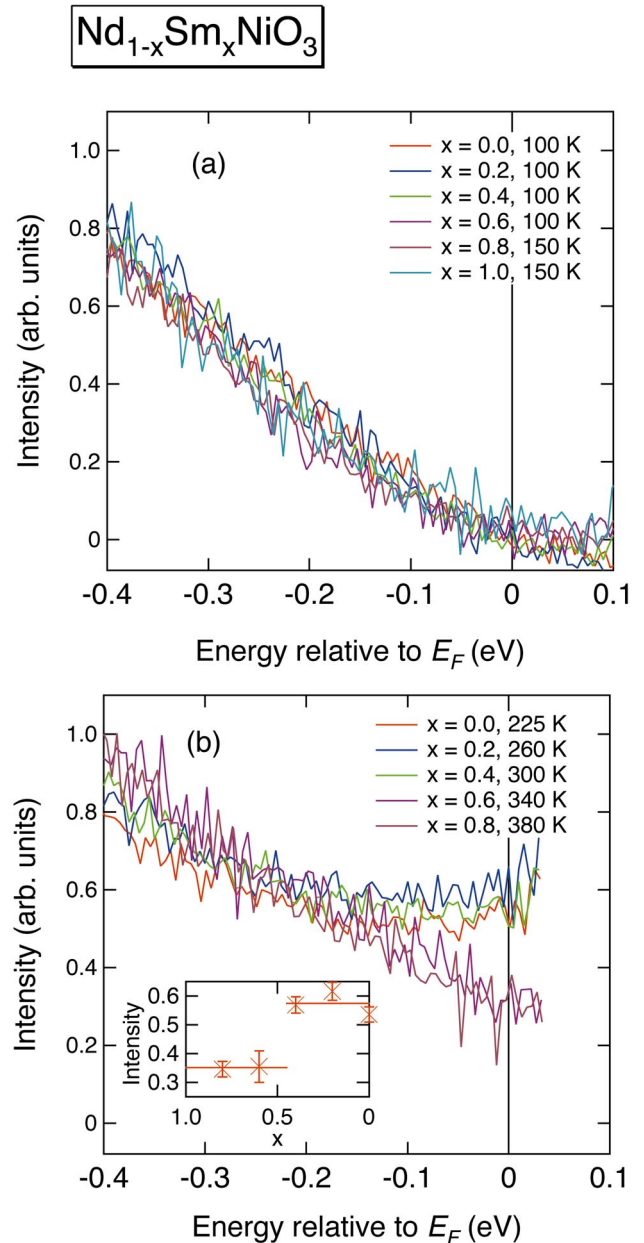


FIG. 4. (Color) Composition dependence of the photoemission spectra $\text{Nd}_{1-x}\text{Sm}_x\text{NiO}_3$. (a) Spectra taken at the lowest temperatures. (b) Spectra taken just above T_{MI} . The inset shows the normalized intensity at E_F just above T_{MI} as a function of x .

by 4.4 K. A similar amount of deviation was also observed by Frand *et al.*¹² This small uncertainty in T_{MI} , however, does not affect our following discussions, as our data points correspond to temperatures which are far above or far below this uncertainty range. Oxygen stoichiometry was determined by the thermogravimetric analysis for Nd and Sm samples and the compositions were found to be $\text{NdNiO}_{3.01}$ and $\text{SmNiO}_{2.99}$, respectively. Since intermediate compositions were synthesized under the same conditions as the end members, the oxygen stoichiometry in these compositions also should be similar. Photoemission measurements were carried out using a VSW hemispherical analyzer and a VG He discharge lamp. The He I (21.2 eV) resonance line was

used for excitation. The total-energy resolution was set to about 30 meV. Clean surfaces were obtained by repeated *in situ* scraping at each measurement temperature. The base pressure of the spectrometer was better than 1×10^{-10} Torr.

Figure 2 shows the photoemission spectra of $\text{Nd}_{1-x}\text{Sm}_x\text{NiO}_3$ at various temperatures. All the spectra have been normalized to the integrated intensity in the indicated energy range, that is, from -0.8 to 0.2 eV. The results for NdNiO_3 and SmNiO_3 are consistent with Vobornik *et al.* results,¹⁰ i.e., the spectra of NdNiO_3 show a high intensity at E_F above T_{MI} and decreasing intensity below T_{MI} . The intensity decreases continuously with decreasing temperature even well below T_{MI} . The intensity in the range $-(0.3-0.7)$ eV, on the other hand, increases with decreasing temperature indicating spectral weight transfer from $-(0-0.3)$ to $-(0.3-0.7)$ eV. The spectra of SmNiO_3 show a weaker temperature dependence below T_{MI} . As for the intermediate compositions, the spectra show a finite spectral weight transfer from the region $-(0-0.3)$ to $-(0.3-0.7)$ eV, although its strength is intermediate between $x=0.0$ and $x=1.0$. In order to remove the effect of the Fermi-Dirac distribution function and deduce the experimental “density of states” (DOS), we have divided the spectra by the Fermi-Dirac distribution function broadened with a Gaussian corresponding to the experimental resolution as shown in the inset of each panel of Fig. 2. For $x \leq 0.4$, the experimental DOS above T_{MI} is almost flat or weakly increases with energy. Below T_{MI} , the DOS at E_F gradually decreases with decreasing temperature. On the other hand, the spectra for $x > 0.4$ is pseudogaplike already above T_{MI} . Figure 3 shows the temperature dependence of the averaged intensity within 0.05 eV of E_F normalized in the same way as in Fig. 2. This figure brings out different behavior of the regions $x \leq 0.4$ and $x > 0.4$. Because of the pseudogap, the averaged intensity for $x > 0.4$ is nearly half compared to that for $x \leq 0.4$ just above T_{MI} . On the other hand, intensity jump at T_{MI} is almost the same between $x \leq 0.4$ and $x > 0.4$.

Figure 4 shows the Fermi-Dirac function-divided spectra taken at the lowest temperatures and just above T_{MI} . The spectra taken at the lowest temperatures are nearly identical for all x 's. This suggests that the ground state is essentially the same for all x 's, i.e., in the same antiferromagnetic insulating state.¹³ On the other hand, the spectra above T_{MI} are quite different between $x \leq 0.4$ and $x > 0.4$. The spectra for $x \leq 0.4$ are nearly flat around E_F whereas the ones for $x = 0.6$ and 0.8 show a weak pseudogaplike behavior. This indicates that the paramagnetic metallic phase is different between $x \leq 0.4$ and $x > 0.4$. As shown in the inset of Fig. 4(b), the averaged intensity within 0.05 eV of E_F just above T_{MI} changes at $x \sim 0.4$. Here, the intensity has been normalized in the same way as Figs. 2 and 3. From these results, we consider that a phase boundary or a crossover line exists within the high-temperature metallic phase at $x \sim 0.4$.

There have been some reports which indicate that the metallic phase may be different between NdNiO_3 and SmNiO_3 . According to the magnetic susceptibility measurement of NdNiO_3 (Ref. 18) and SmNiO_3 ,¹⁹ the metallic phase of

NdNiO_3 is Pauli paramagnetic after the subtraction of the rare-earth local-moment contribution, while that of SmNiO_3 is Curie-Weiss like. This result would indicate that the metallic phase of NdNiO_3 is essentially the same as that of Pauli-paramagnetic LaNiO_3 , while conduction electrons in the metallic phase of SmNiO_3 show local moment behavior. Due to the existence of the fluctuating local moment, the metallic phase of SmNiO_3 would have a large magnetic entropy. If the entropy of the local moments plus that of the conduction electrons in the metallic phase exceed the entropy of the local moments in the paramagnetic insulating phase, the metallic phase can exist on the higher temperature side of the paramagnetic insulating phase across the first-order metal-insulator phase boundary. In the $\text{Nd}_{1-x}\text{Sm}_x\text{NiO}_3$ system, the bandwidth becomes narrower with Sm content, making Δ/W larger. We propose that with Sm content, the Ni $3d$ electrons become more strongly correlated and the local magnetic moment is formed.

Finally, we comment on the origin of the strong temperature dependence of the spectra in the insulating phase. Granados *et al.*^{20,21} and Blasco and Garcia²² have reported that hysteresis below T_{MI} extends to a wide temperature range up to 70 K from the transport and calorimetric measurements and proposed that the metallic and insulating phases coexist over this temperature range. The temperature dependence of the photoemission spectra in the insulating phase may be related to this unusually strong hysteresis. We may attribute these strong hysteretic features to the coexistence of the two phases caused by disorder such as oxygen nonstoichiometry and/or rare-earth atom vacancies, which cannot be avoided in this kind of materials.²³ In a system where both disorder and electron correlation effect are important, the spectra may show an unusual temperature dependence as reported by Sarma *et al.*²⁴ on disorder-induced metal-insulator transition in $\text{LaNi}_{1-x}\text{M}_x\text{O}_3$ ($M = \text{Mn}, \text{Fe}, \text{and Co}$). According to them, while an insulating compound has a finite gap at E_F at very low temperatures, the gap closes at elevated temperature. Competing or cooperative behaviors between electron correlation and disorder have not been investigated so far and have to be clarified in the future.

In conclusion, we have studied the temperature-dependent electronic structure of $\text{Nd}_{1-x}\text{Sm}_x\text{NiO}_3$ by photoemission measurements. While the spectra at the lowest temperatures are identical for all x 's, the spectra above T_{MI} show a pseudogap behavior for $x > 0.4$, different from the spectra of a typical metal for $x \leq 0.4$. It appears that the appearance of the pseudogap is related with the appearance of local magnetic moment in the metallic phase of $x > 0.4$. We propose that the nature of the metallic state is different between these two composition ranges caused by a change in the strength of electron correlation between the two regions.

The authors would like to thank D. D. Sarma for enlightening discussion. This work was supported by Grants-in-Aid for Scientific Research A12304018 and “Novel Quantum Phenomena in Transition Metal Oxides” from the Ministry Education, Culture, Sports, Science, and Technology. J.A.A. and M.J.M.L. acknowledge the Spanish Ministry of Science and Technology for funding the Project MAT 2001-0539.

- ¹N. F. Mott, *Metal-insulator Transitions* (Taylor and Francis, London/Philadelphia, 1990).
- ²M. Imada, A. Fujimori, and Y. Tokura, *Rev. Mod. Phys.* **70**, 1039 (1998).
- ³A. Georges, G. Kotliar, W. Kraith, and M.J. Rozenberg, *Rev. Mod. Phys.* **68**, 13 (1996).
- ⁴H. Takano and A. Okiji, *J. Phys. Soc. Jpn.* **50**, 3835 (1981).
- ⁵D.B. McWhan, J.P. Remeika, T.M. Rice, W.F. Brinkman, J.P. Maita, and A. Menth, *Phys. Rev. Lett.* **27**, 941 (1971); D.B. McWhan, A. Menth, J.P. Remeika, W.F. Brinkman, J.P. Maita, and A. Menth, *Phys. Rev. B* **7**, 1920 (1973).
- ⁶J.A. Wilson and G.D. Pitt, *Philos. Mag.* **23**, 1297 (1971); G. Czjzek, J. Fink, H. Schmidt, G. Krill, M.F. Lapierre, P. Paissod, F. Gautier, and C. Robert, *J. Magn. Magn. Mater.* **3**, 58 (1976).
- ⁷J.B. Torrance, P. Lacorre, A.I. Nazzal, E.J. Ansaldo, and Ch. Niedermayer, *Phys. Rev. B* **45**, 8209 (1992).
- ⁸J. Zaanen, G.A. Sawatzky, and J.W. Allen, *Phys. Rev. Lett.* **55**, 418 (1985).
- ⁹J. B. Goodenough and J. M. Longe, *Magnetic and Other Properties in Oxides and Related Compounds*, edited by K. H. Hellwege and A. M. Hellwege, Landolt-Börnstein, New Series, Group III, Vol. 4, pt. a (Springer-Verlag, Berlin, 1970).
- ¹⁰I. Vobornik, L. Perfetti, M. Zacchigna, M. Grioni, G. Margaritondo, J. Mesot, M. Medarde, and P. Lacorre, *Phys. Rev. B* **60**, R8426 (1999).
- ¹¹R. Mallik, E.V. Sampathkumaran, J.A. Alonso, and M.J. Martínez-Lope, *J. Phys.: Condens. Matter* **10**, 3969 (1998).
- ¹²G. Frand, O. Bohnke, P. Lacorre, J.L. Lourquet, A. Carré, B. Eid, J.G. Théobald, and A. Gire, *J. Solid State Chem.* **120**, 157 (1995).
- ¹³This is consistent with the fact that the magnetic structure is the same between NdNiO₃ (Ref. 14) and SmNiO₃ (Ref. 15). Also, charge disproportionation was recently found in NdNiO₃ (Ref. 16), which implied that it is present in all RNiO₃ ($R \neq \text{La}$) because it had been already found in other RNiO₃ with small R ($R = \text{Ho, Y, Er, Tm, Yb, and Lu}$) (Ref. 17).
- ¹⁴J.L. García-Muñoz, J. Rodríguez-Carvajal, and P. Lacorre, *Phys. Rev. B* **50**, 978 (1994).
- ¹⁵J. Rodríguez-Carvajal, S. Rosenkranz, M. Medarde, P. Lacorre, M.T. Fernández-Díaz, F. Fauth, and V. Trounov, *Phys. Rev. B* **57**, 456 (1998).
- ¹⁶M. Zaghrioui, A. Bulou, P. Lacorre, and P. Laffez, *Phys. Rev. B* **64**, 081102(R) (2001).
- ¹⁷J.A. Alonso, J.L. García-Muñoz, M.T. Fernández-Díaz, M.A.G. Aranda, M.J. Martínez-Lope, and M.T. Casais, *Phys. Rev. Lett.* **82**, 3871 (1999); J.A. Alonso, M.J. Martínez-Lope, M.T. Casais, J.L. García-Muñoz, and M.T. Fernández-Díaz, *Phys. Rev. B* **61**, 1756 (2000); J.A. Alonso, M.J. Martínez-Lope, M.T. Casais, J.L. García-Muñoz, M.T. Fernández-Díaz, and M.A.G. Aranda, *ibid.* **64**, 094102 (2001).
- ¹⁸J. Pérez, J. Stankiewicz, J. Blasco, M. Castro, and J. García, *J. Phys.: Condens. Matter* **8**, 10393 (1996).
- ¹⁹J. Pérez-Cacho, J. Blasco, J. García, M. Castro, and J. Stankiewicz, *J. Phys.: Condens. Matter* **11**, 405 (1999).
- ²⁰X. Granados, J. Fontcuberta, X. Obradors, and J.B. Torrance, *Phys. Rev. B* **46**, 15 683 (1992).
- ²¹X. Granados, J. Fontcuberta, X. Obradors, Ll. Mañosa, and J.B. Torrance, *Phys. Rev. B* **48**, 11 666 (1993).
- ²²J. Blasco and J. García, *J. Phys.: Condens. Matter* **6**, 10 759 (1994).
- ²³A. Moreo, M. Mayr, A. Feiguin, S. Yunoki, and E. Dagotto, *Phys. Rev. Lett.* **84**, 5568 (2000).
- ²⁴D.D. Sarma, A. Chainani, S.R. Krishnakumar, E. Vescovo, C. Carbone, W. Eberhardt, O. Rader, Ch. Jung, Ch. Hellwig, W. Gudat, H. Srikanth, and A.K. Raychaudhuri, *Phys. Rev. Lett.* **80**, 4004 (1998).